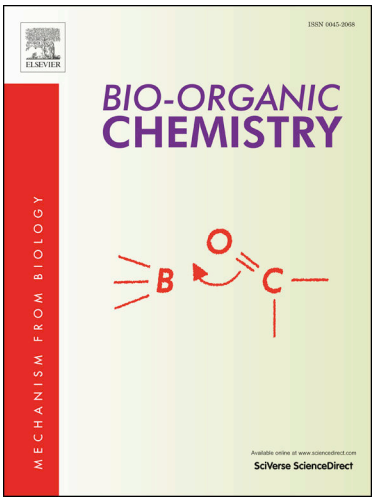


# Flavonoid derivatives synthesis and anti-diabetic activities

Ying Chen, Feng-Bo Cheng, Xiao-Ran Wu, Wen Zhu, Jian-Wen Liao, Yue Jiang, Chang Zhang, Wen-Yan Niu, Yang Yu, Hong-Quan Duan, Nan Qin

PII: S0045-2068(19)31367-7
DOI: https://doi.org/10.1016/j.bioorg.2019.103501
Reference: YBIOO 103501

To appear in: *Bioorganic Chemistry*

Received Date: 28 August 2019
Revised Date: 30 October 2019
Accepted Date: 7 December 2019

Please cite this article as: Y. Chen, F-B. Cheng, X-R. Wu, W. Zhu, J-W. Liao, Y. Jiang, C. Zhang, W-Y. Niu, Y. Yu, H-Q. Duan, N. Qin, Flavonoid derivatives synthesis and anti-diabetic activities, *Bioorganic Chemistry* (2019), doi: https://doi.org/10.1016/j.bioorg.2019.103501

# Flavonoid derivatives synthesis and anti-diabetic activities

Ying Chen[1], Feng-Bo Cheng[1], Xiao-Ran Wu[1], Wen Zhu[1,2], Jian-Wen Liao[1,3], Yue Jiang[1,2], Chang Zhang[1], Wen-Yan Niu[4], Yang Yu[1], Hong-Quan Duan[1,5*], and Nan Qin[1*]

[1]School of Pharmacy, Tianjin Medical University, Tianjin Key Laboratory on Technologies Enabling Development Clinical Therapeutics and Diagnostics (Theragnostic), Tianjin, People's Republic of China

[2]Department of Pharmacy, Tianjin Children's Hospital, People's Republic of China

[3]Tianjin Neurosurgery Institute, Tianjin Cerebral Vascular and Neural Degenerative Disease Key Laboratory, Tianjin Huanhu Hospital, Tianjin, People's Republic of China

[4]Department of Immunology, Key Laboratory of Immune Microenvironment and Disease of the Educational Ministry of China, People's Republic of China

[5]Research Center of Basic Medical Sciences, Tianjin Medical University, Tianjin, People's Republic of China

Corresponding authors:

Hong-Quan Duan, duanhq@tmu.edu.cn

Nan Qin, qinnan@tmu.edu.cn

**Abstract**

In high fat diet-induced obese mice, the flavonoid derivative of tiliroside, Fla-CN, has antihyperglycemic effects, can improve insulin sensitivity, ameliorate metabolic lipid disorders, and benefits certain disorders characterized by insulin resistance. Fla-CN is a novel lead compound to discovery anti-diabetic and anti-obesity drugs. The present study reported the optimization of Fla-CN to obtain a new derivative, **10b**, which has improved glucose consumption at the nanomolar level ($EC_{50}$ = 0.3 nM) in insulin resistant (IR) HepG2 cells. **10b** also increased the glycogen content and glucose uptake, and concurrently inhibited gluconeogenesis in HepG2 cells. Western blotting showed that **10b** markedly enhanced the phosphorylation of AMPK (AMP-activated protein kinase) and AS160 (protein kinase B substrate of 160 kDa) and reduced the levels of the gluconeogenesis key enzymes PEPCK (phosphoenolpyruvate carboxykinase) and G6P (glucose 6-phosphatase) in HepG2 cells. The potential molecular mechanism of **10b** may be activation of the AMPK/AS160 and AMPK/PEPCK/G6P pathways. We concluded that **10b** might be a valuable candidate to discover anti-diabetic drugs.

**Keywords:** Flavonoids, Structure-Activity Relationship, Glucose Metabolism Disorders, ratio of AMP/ATP, AMPK pathway

## 1. Introduction

Hyperglycemia is driven by impaired rates of peripheral glucose uptake and elevated rates of hepatic glucose output. The production of glucose is one of the most important functions of the liver. This process is under complex control by substrates, hormones, and nerves [1]. This control is achieved by diverse regulatory mechanisms that tune the activities of enzymes and transporters in a concerted fashion. In the rat liver, significant changes in the carbohydrate metabolism-related enzyme levels occur between 5 and 100 hours during a starvation-refeeding cycle [2, 3]. In a given metabolic system, not all enzymes are equally important for the regulation of systemic behavior. Rather, only specific key enzymes carry the burden of regulatory control. For example, glucose-6-phosphatase (G6P) and phosphoenolpyruvate carboxykinase (PEPCK), which have the key roles in hepatic glucose production regulation and could be applied therapeutically to treat hyperglycemia. AMP-activated protein kinase (AMPK) is an energy-sensing enzyme that controls glucose and lipid metabolism. AMPK activation increases glucose uptake, fatty acid oxidation, and mitochondrial biogenesis, which helps to ameliorate different aspects of metabolic dysregulation, including hyperglycemia and insulin resistance [4]. Therefore, to overcome chronic diabetes, researchers are seeking novel classes of anti-hyperglycemia factors with multiple effects or targets.

A semi-synthesized flavonoid derivative of tiliroside, 3-O-[(E)-4-(4-cyanophenyl)-2-oxobut-3-en-1-yl]kaempferol (Fla-CN, Fig. 1), caused significantly enhanced glucose consumption compared with that of metformin in HepG2 cells, which are an insulin-resistant (IR) human hepatocellular carcinoma cell line [5]. An *in vivo* study in high fat diet induced obese mice showed that Fla-CN had antihyperglycemic effects, could improve insulin sensitivity, ameliorate metabolic lipid disorders, and benefit certain disorders characterized by insulin resistance [6]. The present study investigated the structural optimization of Fla-CN to obtain the new derivatives with enhanced effects on glucose metabolism. Furthermore, we explored that the possible molecular mechanism of the activity of Fla-CN derivatives.

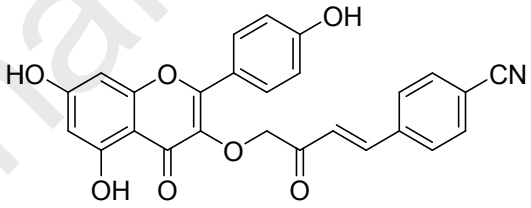


**Fig. 1 The chemical structure of**

**3-O-[(E)-4-(4-cyanophenyl)-2-oxobut-3-en-1-yl]kaempferol (Fla-CN)**

## 2. Results

### 2.1 Chemistry

Derivatives of Fla-CN were synthesized according to a previous report with some major adaptations [5]. All derivatives were prepared through aldol

condensation. In comparison with our earlier study, morpholinium trifluoroacetate was used to catalyze this aldol condensation, with reference to Zumbansen's report[7]. To obtain alkynyl substituted derivatives **4a-4d**, a Sonogashira reaction was used in the first step (Scheme 1). Nitrogen heterocycle derivatives **8h-8u** and **10a-10b** were synthesized using building blocks **9h-9u,** which were constructed from fluorine-substituted formylbenzonitrile (Scheme 2).

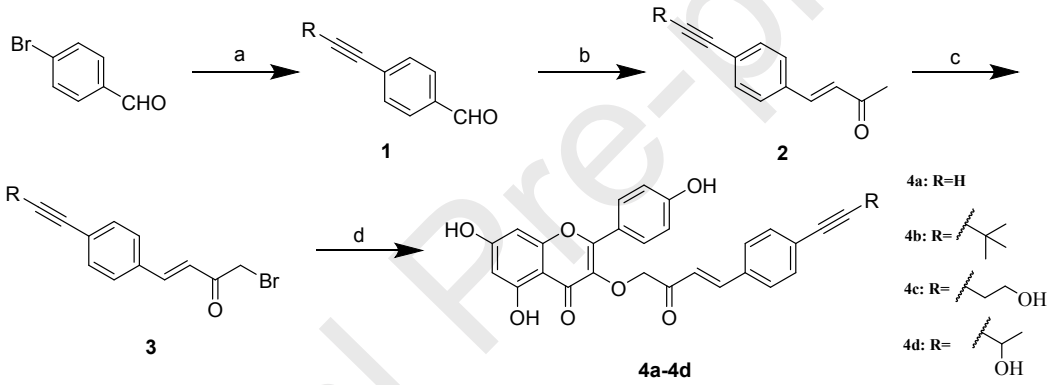


Reagents and conditions: a.alkyne, $Pd(PPh_3)_2Cl_2$, CuI, TEA,THF, r.t.; b. Morpholine TFA salts, acetone, reflux; c.Pyrrolidone hydrotribromide, THF, r.t.; d. Kaempferol, $K_2CO_3$, 1,4-dioxane, 80°C;

**Scheme 1. Synthesis of compounds 4a-4d**

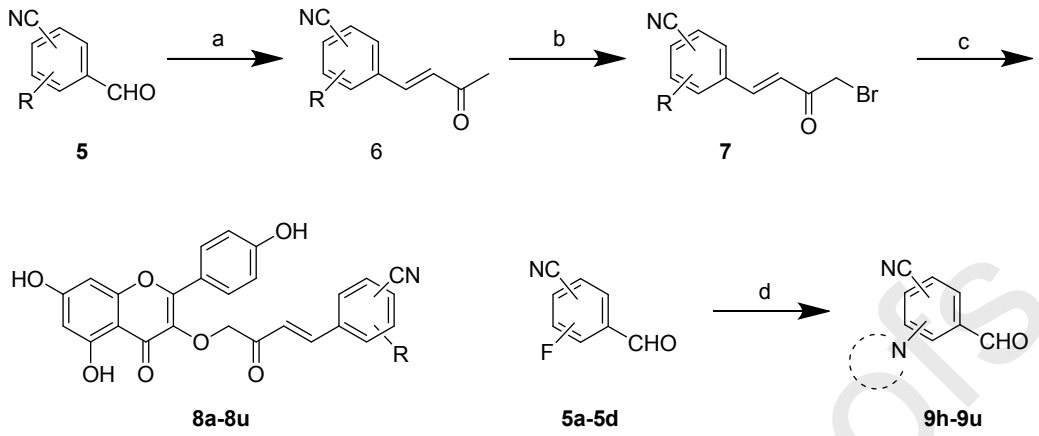


Reagents and conditions: a. Morpholine TFA salts, acetone, reflux; b. Pyrrolidone hydrotribromide, THF, r.t.; c. Kaempferol, $K_2CO_3$, 1,4-dioxane, 80°C; d. amine, $K_2CO_3$, THF, 65°C.

| No. | Substituted Group | No. | Substituted Group | No. | Substituted Group |
|---|---|---|---|---|---|
| **8a** | 2-F,4-CN | **8h** | 2-pyrrolidinyl,4-CN | **8o** | 3-CN,4-piperidinyl |
| **8b** | 2-F,5-CN | **8i** | 2-pyrrolidinyl,5-CN | **8p** | 2-morpholinyl,4-CN |
| **8c** | 3-F,4-CN | **8j** | 3-pyrrolidinyl,4-CN | **8q** | 2-morpholinyl,5-CN |
| **8d** | 3-CN,4-F | **8k** | 3-CN,5-pyrrolidinyl | **8r** | 3-morpholinyl,4-CN |
| **8e** | 3-F,5-CN | **8l** | 2-piperidinyl,4-CN | **8s** | 3-CN,4-morpholinyl |
| **8f** | 2-Cl,3-CN | **8m** | 2-piperidinyl,5-CN | **8t** | 2-(N-Boc-piperazineyl),4-CN |
| **8g** | 2-Cl,5-CN | **8n** | 3-piperidinyl,4-CN | **8u** | 2-(N-Boc-piperazineyl),5-CN |

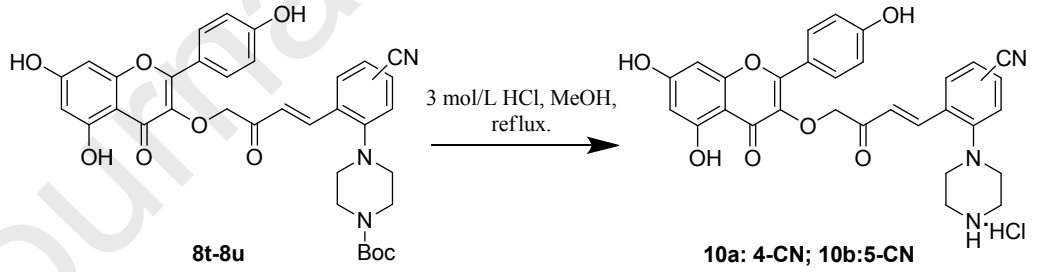


**Scheme 2. Synthesis of compounds 8a-8u and 10a-10b**

## 2.2 Pharmacology

### 2.2.1 Effects of the flavonoid derivatives on glucose consumption

The glucose consumption of IR HepG2 cells in response to all the derivatives

were evaluated and $EC_{50}$ values were used to assess their potencies. Compounds **4b-4d**, **8a-8s**, and **10a-10b** significantly enhanced glucose consumption in IR HepG2 cells (Table 1). In this optimization study, four derivatives (**4b, 8m, 10a**, and **10b**) showed higher potency than the lead compound Fla-CN. The chemical structure of **4b** was different from the other three compounds; therefore, **4b** and **10b** were chosen for the more detailed research associated with glucose metabolism.

**Table 1. Effects of Fla-CN derivatives on IR HepG2 cells' glucose consumption (n = 3).**

| No. | $EC_{50}$ (nM) | No. | $EC_{50}$ (nM) | No. | $EC_{50}$ (nM) |
|---|---|---|---|---|---|
| **4a** | 63.9 ± 8.59 | **8g** | 10.8 ± 1.46 | **8q** | 1.5 ± 0.34 |
| **4b** | 0.4 ± 0.11 | **8h** | 8.3 ± 0.93 | **8r** | 8.7 ± 1.33 |
| **4c** | 9.3 ± 1.63 | **8i** | 6.1 ± 0.87 | **8s** | 7.6 ± 1.38 |
| **4d** | 15.1 ± 1.57 | **8j** | 11.8 ± 1.38 | **8t** | 52.3 ± 7.62 |
| **8a** | 1.2 ± 0.36 | **8k** | 18.3 ± 2.36 | **8u** | 45.2 ± 6.61 |
| **8b** | 2.3 ± 0.49 | **8l** | 1.8 ± 0.27 | **10a** | 0.8 ± 0.36 |
| **8c** | 6.5 ± 0.74 | **8m** | 0.9 ± 0.15 | **10b** | 0.3 ± 0.07 |
| **8d** | 5.9 ± 0.77 | **8n** | 10.1 ± 1.28 | **Fla-CN** | 3.3 ± 0.54 |
| **8e** | 5.0 ± 0.85 | **8o** | 9.5 ± 1.31 | **Met** | 258.1 ± 33.36 |
| **8f** | 5.4 ± 0.65 | **8p** | 1.2 ± 0.67 | | |

Our previous study found that the cyan-substituted flavonoid derivative (Fla-CN) showed potential anti-diabetic activity [5]. Cyan groups contain C-N triple bonds; therefore, our first thought was to substitute C-N triple bonds by C-C triple bonds. Based on this notion, **4a-4d** were designed, synthesized, and evaluated for their activities. Compared with other alkyne-containing derivatives, **4b** exhibited higher activity than Fla-CN (Table 1). Combining the results of **4a-4d** and those of a previous study[5], we speculated that the cyan group was the most active group. Halogen bonding had been successfully harnessed for lead identification and optimization [8]; therefore, multi substituted groups, such as a fluorine atom or chlorine atom, were introduced into the Fla-CN derivatives that also contained a cyan group (**8a**-**8g**). Most of these derivatives exhibited the same effects as Fla-CN at the same order of magnitude. Moreover, the results showed that the effects had good tolerance at the substituted positions of the cyan groups. Aromatic amines usually appear in marketed drugs; therefore, a C-N bond was also introduced into Fla-CN (**8h**-**8s**) to discover more potent derivatives. Fortunately, six-membered heterocyclic nitrogen derivatives at the 2-subsititued position (**8l, 8m 8p**, and **8q**) exhibited higher activities than Fla-CN (Table 1). Based on this discovery, we designed other two six-membered heterocyclic nitrogen derivatives at the 2-subsititued position (**10a** and **10b**). To our surprise, both **10a** and **10b** showed higher potency, with $EC_{50}$ values below 1.0 nM (Table 1).

### 2.2.2 Effects of the flavonoid derivatives on glucose uptake

To investigate whether flavonoid derivatives could promote glucose uptake in HepG2 cells, we evaluated the uptake of 2-NBDG (2-(N-(7-Nitrobenz-2-oxa-1,3-diazol-4-yl)Amino)-2-Deoxyglucose) by HepG2 cells treated with different concentrations of **Fla-CN**, **4b**, **10b**, and insulin (Fig. 2A–C). Compared with that of the control group, the cells treated with **Fla-CN**, **4b**, and **10b** showed significantly enhanced 2-NBDG uptake, in a dose-dependent manner ($P < 0.05$).

## 2.3 Effects of the flavonoid derivatives on the glycogen content

Compared with that of the control group, the glycogen content in the insulin-treated group was significantly increased ($P < 0.001$). Compared with the control group, **4b** at 12.5 μM effectively increased the glycogen content ($P < 0.01$) in HepG2 cells (Fig. 2E). Compared with the control group, **10b** and **Fla-CN** also effectively increased the glycogen content (2.5 μM, $P < 0.01$; 12.5 μM, $P < 0.001$, respectively) in HepG2 cells (Fig. 2D, F). These results suggested that **4b**, **10b**, and **Fla-CN** promoted glycogen synthesis, supporting the hypothesis that treatment with these flavonoid derivatives improved glucose metabolism in HepG2 cells.

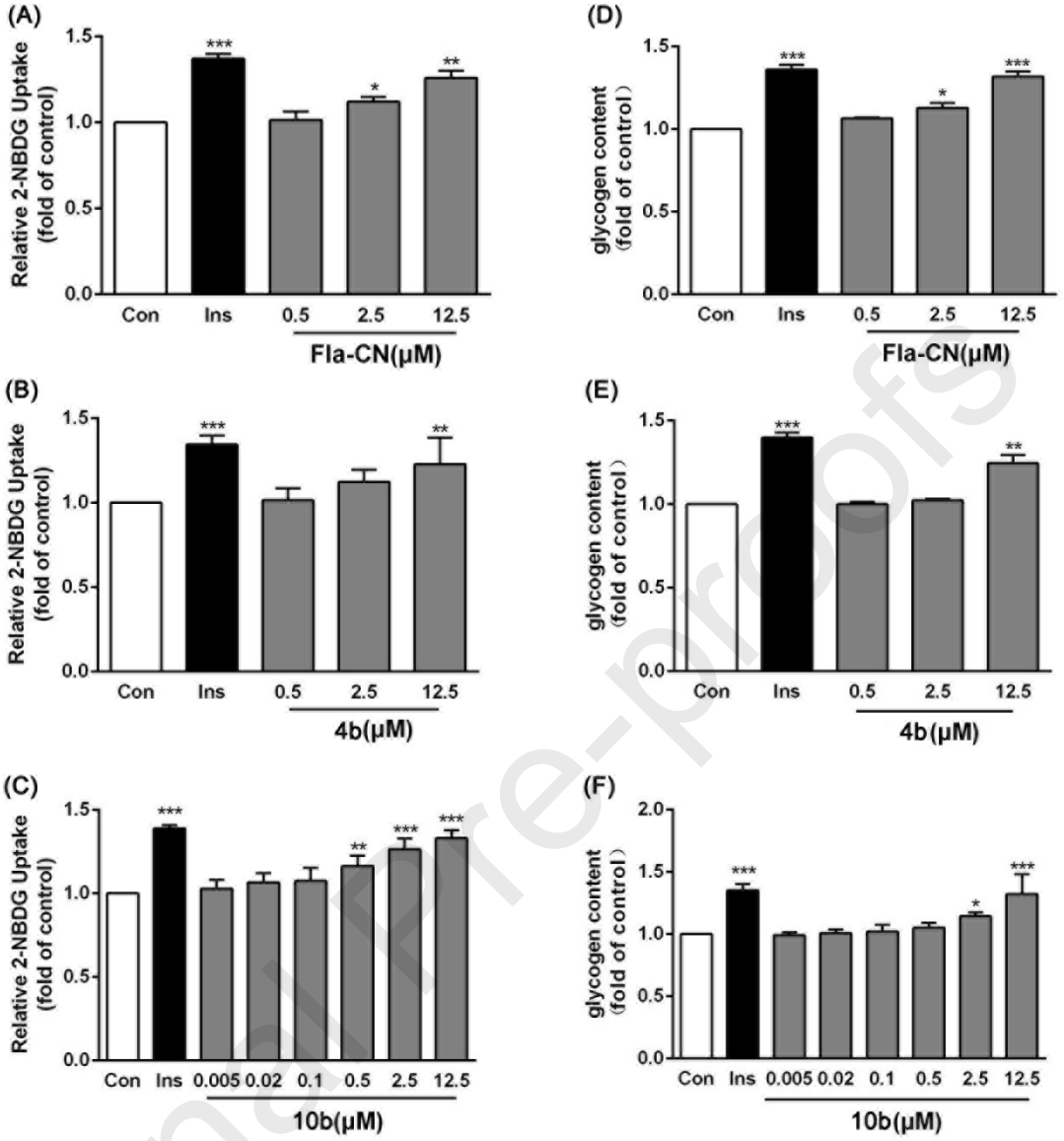


**Fig. 2 The effects of Fla-CN derivatives on glucose uptake and the glycogen content.** The effects on glucose uptake of Fla-CN (A), 4b (B), and 10b (C) in HepG2 cells. Glucose uptake activity was measured using fluorescent 2-NBDG (2-(N-(7-Nitrobenz-2-oxa-1,3-diazol-4-yl)Amino)-2-Deoxyglucose). The effects of Fla-CN (D), 4b (E) and 10b (F) on the glycogen contents of HepG2 cells. Data represent the mean ± the standard error of the mean (SEM); n = 4. ($^{*}P < 0.05$, $^{**}P < 0.01$, $^{***}P < 0.001$ compared with the control group).

### 2.3.1 Effects of the flavonoid derivatives on gluconeogenesis

Fig. 3A–C shows that metformin, a prescription drug, decreased glucose production at 1.0 mM ($P < 0.01$). **Fla-CN** also decreased glucose production at 2.5 ($P < 0.05$) and 12.5 μM ($P < 0.001$), respectively (Fig. 3A). Derivative **4b** decreased glucose production only at 12.5 μM ($P< 0.01$, Fig. 3B). Fig. 3C shows that **10b** treatment resulted in decreased glucose production in a dose dependent manner.

### 2.3.2 Effects on the flavonoid derivatives on glycolysis

To investigate the effects of **4b**, **10b**, or **Fla-CN** on anaerobic respiration, lactate release from HepG2 hepatocytes was measured. Insulin at 100 nM was used as positive control. HepG2 cells were treated for 24 h with 0.5, 2.5, 12.5 mmol/L **4b**, **10b** or **Fla-CN** (together with no compound controls). Lactate release from HepG2 hepatocytes was increased by insulin ($P < 0.001$; Fig. 3D–F). The concentration of lactate showed no significant difference between flavonoid derivatives and the control group (Fig. 3D–3F). Lactate is the end product of glycolysis; therefore, these data suggested that **4b**, **10b**, or **Fla-CN** did not affect glycolysis.

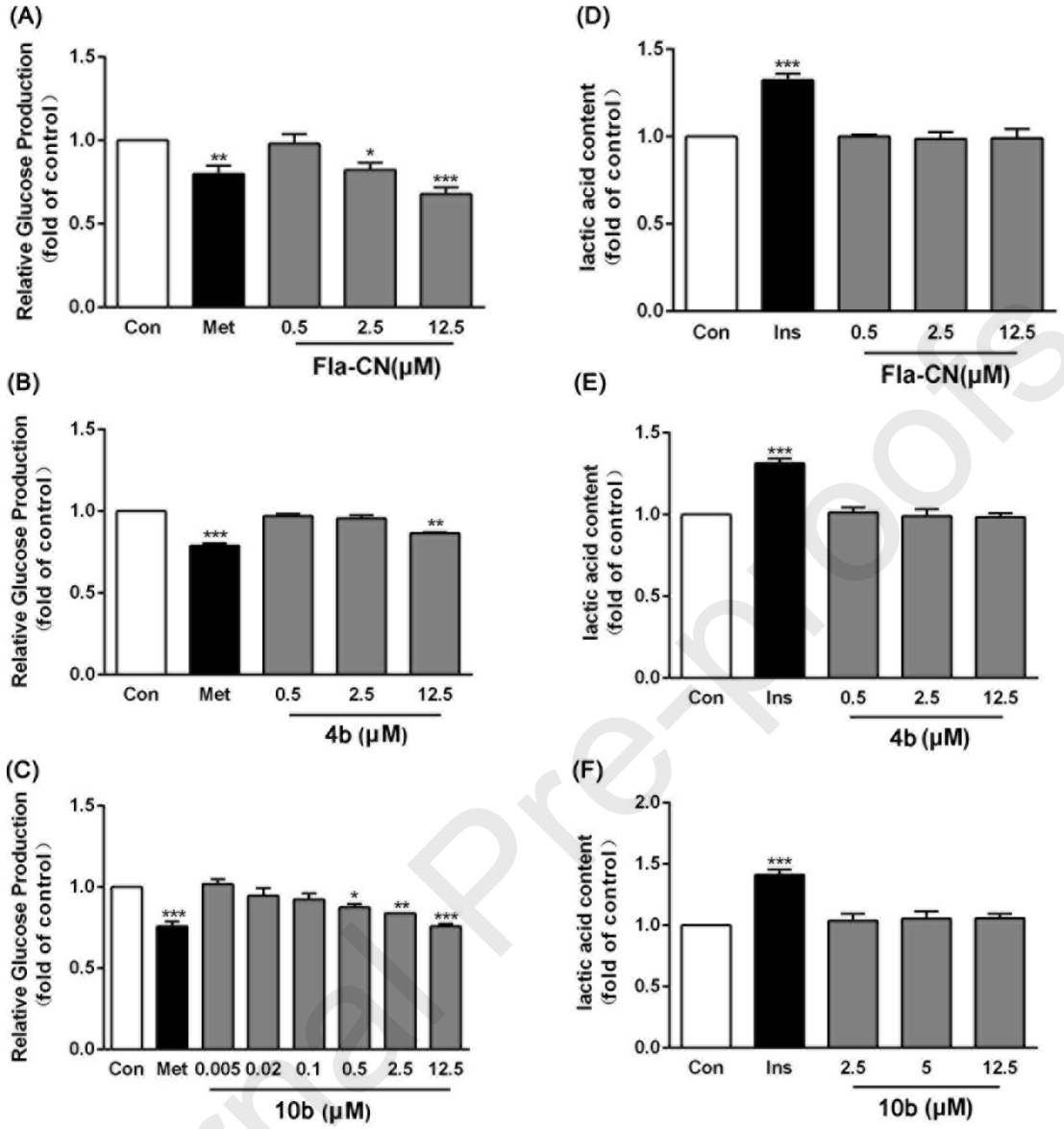


**Fig. 3 The effects of Fla-CN derivatives on gluconeogenesis and glycolysis.** The effects on gluconeogenesis of Fla-CN (A), 4b (B), and 10b (C) in HepG2 cells. The effects on glycolysis of Fla-CN (D), 4b (E) and 10b (F) in HepG2 cells. Data represent the mean ± the standard error of the mean (SEM); n = 4. ($^{*}P < 0.05$, $^{**}P < 0.01$, $^{***}P < 0.001$ compared with the control group).

## 2.4 Potential molecular mechanism on glucose metabolism in response to of flavonoid derivative 10b

The above evaluations of **Fla-CN**, **4b** and **10b** suggested that **10b** exhibited more potency than **Fla-CN** and **4b** on glucose metabolism. Fla-CN activated AMPK *in vitro* and *in vivo* [7,8]; therefore, AMPK may be a key factor in the molecular mechanism of glucose metabolism. As shown in Fig. 4, in HepG2 cells, **10b** treatment at 0.5 to 12.5 μM led to markedly enhanced levels of phosphorylated AMPK and AS160 (protein kinase B substrate of 160 kDa) compared with those of the control group, in a dose dependent manner.

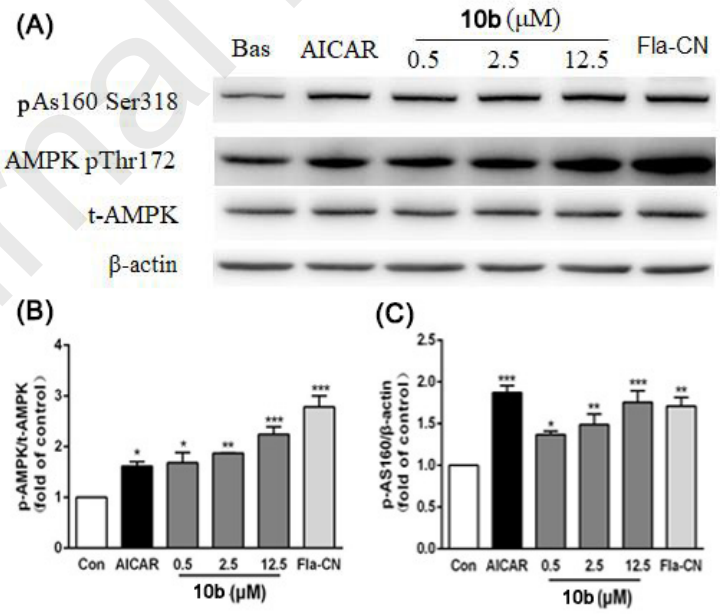


**Fig. 4 The effects of 10b on the levels of AMPK, phospho (p)-AMPK and p-AS160 in HepG2 cells.** The positive control comprised

5-Aminoimidazole-4-carboxamide 1-β-D-ribofuranoside, (AICAR; 0.1 mM), which is a known activator of AMPK. (A) Western blotting assays detected the levels of AMPK, p-AMPK, AS160, and p-AS160 in HepG2 cells; (B) The relative value of p-AMPK was quantified using densitometry and normalized with that of AMPK; (C) The relative level of p-AS160 was quantified using densitometry and normalized to that of β-actin. Data represent the mean ± the standard error of the mean (SEM); n = 3. ($^{*}P < 0.05$, $^{**}P < 0.01$, $^{***}P < 0.001$ compared with the control group). AMPK, AMP-activated protein kinase; AS160, protein kinase B substrate of 160 kDa.

Phosphoenolpyruvate carboxykinase (PEPCK) and glucose 6-phosphatase (G6P) are key enzymes in gluconeogenesis. The results shown in Fig. 5 indicate that **10b**, Fla-CN, and the AMPK activator AICAR could significantly decrease the protein levels of PEPCK and G6P in HepG2 cells (Fig. 5).

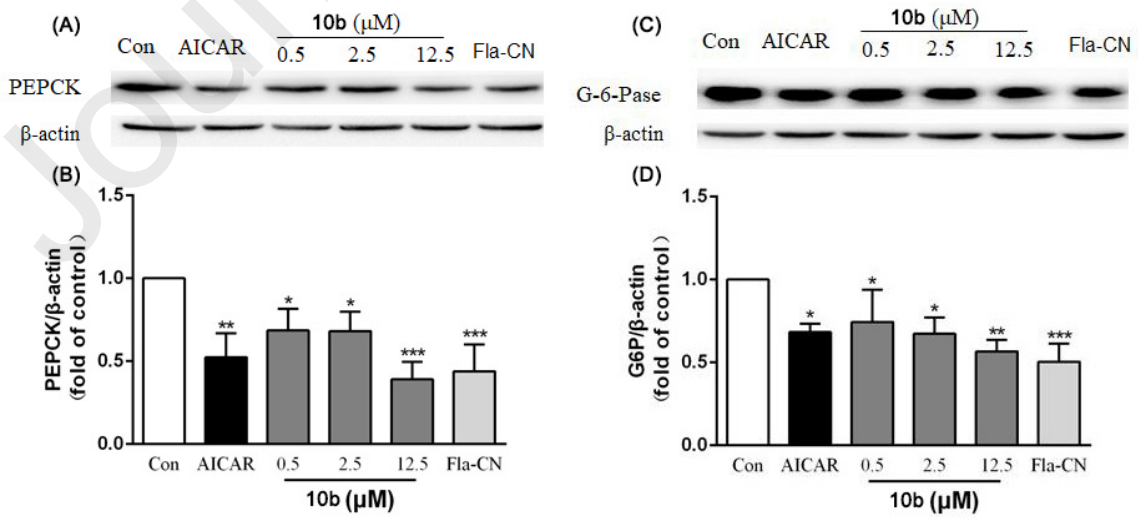


**Fig. 5 The effects of 10b on PEPCK and G6P protein levels in HepG2**

**cells.** (A) Western blotting analysis was used to determine the PEPCK protein levels in HepG2 cells; (B) The relative level of PEPCK was quantified using densitometry and normalized to that of β-actin; (C) Western blotting analysis was used to determine the G6P protein level in HepG2 cells; (D) The relative level of G6P was quantified using densitometry and normalized to that of β-actin. Data represent the mean ± the standard error of the mean (SEM); n = 3. ($^{*}P < 0.05$, $^{**}P < 0.01$, $^{***}P < 0.001$ compared with the control group). PEPCK, phosphoenolpyruvate carboxykinase; G6P, glucose 6-phosphatase (G6P).

## 2.5 Effects of 10b on the AMP/ATP ratio in HepG2 cells

An increase in the ratio of AMP to ATP indicated that several natural compounds and metformin could active AMPK [9-11]. Therefore, we examined the ATP and AMP levels in cultured HepG2 cells after **10b** (10 μM) or vehicle treatment. The results showed that **10b** decreased the ATP content and increased AMP content (Table. 2). Thus, the ratio of AMP to ATP was elevated by treatment with **10b** (Table. 2).

**Table 2. Effects of 10b on the AMP/ATP ratio in HepG2 cells**

| Group | AMP ( $\mu g \cdot mL^{-1}$ ) | ATP ( $\mu g \cdot mL^{-1}$ ) | AMP/ATP |
|---|---|---|---|
| Control | 1.425 ± 0.0423 | 44.942 ± 1.0331 | 0.031/1 |
| **10b** (0.01 μM) | 1.411 ± 0.0382 | 44.120 ± 1.1706 | 0.032/1 |
| **10b** (0.05 μM) | 1.482 ± 0.0195 | 43.508 ± 0.1891 | 0.034/1 |
| **10b** (8 μM) | 1.476 ± 0.0360 | 41.475 ± 0.5798 | 0.036/1* |
| **10b** (12 μM) | 1.670 ± 0.0160 | 42.196 ± 1.0337 | 0.039/1* |

N = 3, $^{*}P < 0.05$ compared with control group

## 3. Discussion

Among all the Fla-CN derivatives, **4b** and **10b** exhibited excellent enhancement of glucose consumption. Furthermore, in the glucose uptake, gluconeogenesis, glycogen production, and glycolysis experiments, both **4b** and **10b** could improve glucose uptake and glycogen production in HepG2 cells (Fig. 2). Meanwhile, these two compounds could inhibit gluconeogenesis in HepG2 cells (Fig. 3A, 3B, 3C). However, neither **4b** nor **10b** affected glycolysis (Fig. 3D–F). Compared with **4b** and **Fla-CN**, **10b** had a lower effective concentration, such as 0.5 or 2.5 μM (Fig. 2C, 2F, 3C).

This phenomenon was attribute to the structural difference of these two derivatives. Compared with **4b** and **Fla-CN**, **10b** has a nitrogen heterocycles fragment. A cursory glance at any of pharmaceutical paper reveals that nitrogen heterocycles are common drug fragments [12]. In this study, five- or six-membered rings were introduced into the lead compound. The results showed that six-membered nitrogen heterocycle derivatives exhibited more potency than five-membered nitrogen heterocycle derivatives (Table 1). The ring size might be a crucial factor for the activity. The binding site of the potential targets might require a larger group at the benzonitrile fragment. Lipophilicity is another underlying structural property that affects higher-level

physicochemical and biochemical properties. It often is an effective guide for modifying the structure of a lead series to improve a property. In this study, the most potency piperazine derivatives **10a** and **10b** exhibit the lowest cLogP values of 3.14 in all of these derivatives. The cLogP value of Fla-CN is 3.30. It was concluded that a lower cLogP might be a better manner of the derivative's activity. Among all the six-membered nitrogen heterocycle derivatives, piperazine derivatives showed excellent potency. This indicated that piperazine is an important group in these derivatives. This was not surprising, because piperazine, as an important nitrogen heterocycle, has been shown to be an essential structural component for many pharmaceuticals. Piperazine derivatives are reported to elicit a broad spectrum of pharmacological activities *viz*. antidepressant, anticancer, anthelmintic, antibacterial, antifungal, antimycobacterial, antimalarial, and anticonvulsant activities [13]. In this study, derivatives **10a** and **10b** exhibited activity at the nanomole levels when they contained a piperazine group. It was possible that the binding pocket of target proteins might have some acidic amino acid residues, some hydrogen bond receptors, or some aromatic amino acid residues. These amino acid residues could interact with the piperazine group. These results were helpful for identifying the binding site of **10b** with its potential target proteins.

AMPK is a highly conserved sensor of cellular energy [4]. A number of pharmacological compounds that increase AMPK activity indirectly, or

through direct binding, have been identified [14]. The first such direct activator to be identified was 5-aminoimidazole-4-carboxamide ribonucleotide (also known as ZMP), the monophosphate derivative of the cell permeable precursor AICAR [15, 16]. This finding led to the wide use of AICAR as a pharmacological tool to investigate the effect of AMPK activation in cells[14]. AMPK is activated in response to an increase in AMP and ADP levels, and this underpins the mechanism of action of a wide number of compounds that indirectly activate AMPK. The biguanide metformin, a widely used oral anti-diabetic drug, inhibits complex I in the mitochondria, leading to a reduction in mitochondrial respiration and ATP production [17]. Metformin has been shown to activate AMPK[9]. A number of plant-derived natural products, which are used in traditional herbal medicine, also activate AMPK indirectly by inhibiting mitochondrial respiration [4], for example, berberine [18] and quercetin [19]. Our previous study reported that a flavonoid derivative could enhance glucose consumption via the AMPK pathway in HepG2 cells [5]. AMPK is a sensor of cellular energy status that becomes activated under conditions of a high cellular AMP/ATP ratio through allosteric binding with AMP and subsequent phosphorylation by upstream AMPK-kinases [20]. Therefore, we analyzed the contents of AMP and ATP levels in **10b** treated HepG2 cells and found that **10b** increased the AMP:ATP ratio in HepG2 cells (Table 2). Thus, derivative **10b** could activate AMPK by increasing the AMP:ATP ratio, as confirmed

using western blotting (Fig. 4). AS160 is also known as a Rab-GTPase activating protein (GAP). The Rab-GAP activity of AS160 maintains Rab substrates in their inactive, GDP-bound, form, which causes intracellular retention of GLUT4 [21]. AS160 phosphorylation by AMPK inactivates its Rab-GAP activity, thereby relieving the inhibition on its Rab substrates. Subsequently, GLUT4 storage vesicles are mobilized to the cell surface under the regulation of activated Rabs [22, 23]. These effects on the AMPK/AS160 pathway might lead directly to enhanced glucose uptake.

Some studies using nonspecific AMPK activators such as AICAR [24, 25] indicated that AMPK repressed key gluconeogenic genes, such as *PEPCK* and *G6P*, both of which have been shown to contribute to aberrant hepatic glucose production in metabolic disorders [26]. In the present study, the AMPK activator AICAR and **10b** could decrease the protein levels of PEPCK and G6P in HepG2 cells (Fig. 5). These results agreed with those of previous study, which demonstrated reduced PEPCK and G6P levels in streptozotocin-induced and ob/ob diabetic mice after adenovirus-induced transfer of constitutively active AMPK [27]. Thus, derivative **10b** might downregulate gluconeogenesis via the AMPK/PEPCK/G6P pathway.

## 4. Conclusion

In the present study, we produced semi-synthesized flavonoid derivatives, most of which could improve glucose consumption in IR HepG2

cells. Among them, **10b** exhibited powerful potency at a nanomolar concentration. Derivative **10b** upregulated glucose uptake and glycogen production, and downregulated gluconeogenesis in HepG2 cells. Its molecular mechanism might be activation the AMPK pathway by upregulating the AMP:ATP ratio. Derivative **10b** could represent a valuable lead compound for the discovery of anti-diabetic drugs. The target identification study of **10b** is undergoing in our lab.

## 5. Experimental section

### 5.1. Chemistry

#### 5.1.1. General instrumentation and reagents

All the solvents and reagents used in the present study came from commercial sources and were used without purification, unless otherwise stated. Reactions were monitored by Thin-layer chromatography (TLC) with precoated silica gel glass plates containing a fluorescence indicator were used to monitor the reactions. Column chromatography was carried out on silica gel ($SiO_2$; 300–400 mesh) and a Toyopeal HW-40 (Tosoh Co., Ltd, Tokyo, Japan). The nuclear magnetic resonance (NMR) spectra were obtained using a Bruker AVANCE III 400 instrument (Bruker, Billerica, MA, USA; $^{1}H$ NMR, 400 MHz; $^{13}C$ NMR, 100 MHz). The high-resolution mass spectra were recorded in ESI mode using an Agilent 1200 LC-MS instrument (Agilent, Palo Alto, CA, USA).

### 5.1.2. General procedure for intermediates synthesis

Compound **1** was prepared in accordance with the Sonogashira coupling reaction [28]. The α, β-unsaturated ketos **2** and **6** were synthesized using morpholine trifluoroacetic acid salts catalyzed by the Classin-Schimitt reaction [7]. The α-bromine substituted ketos **3** and **7** were obtained using pyrrolidone hydrotribromide [5].

### 5.1.3. General procedure for the synthesis of compounds 4 and 8

Target compounds **4** and **8** were semi-synthesized from kaempferol with α-bromine substituted ketos using an etherification reaction. A solution of the bromine substituted ketos (1.0 eq) in 1,4-dioxane (5 ml) was added to a mixture of kaempferol (1.2 eq) and $K_2CO_3$ (1.2 eq) in 1,4-dioxane (10 ml; stirred for 90 min while maintaining gentle reflux) and mixed for 30 min. Stirring of the reaction mixture at 80 °C was continued until TLC indicated that the starting material had disappeared ($CH_2Cl_2$: MeOH, 95:5). Under reduced pressure, the solvent was removed from the reaction mixture, water was added, 1 M HCl was added to the aqueous phase for neutralization (to pH 7), and the reaction was extracted using ethyl acetate. The organic phase was dried over anhydrous magnesium sulfate, filtered, and concentrated. Gel-permeation chromatography (HW-40; $CH_2Cl_2$: MeOH, 1:1) and

preparative-TLC were used to purify the crude product, which appeared as a yellow solid product.

5.1.3.1. 3-O-[(E)-4-(4-ethynyphenyl)-2-oxobut-3-en-1-yl]kaempferol (**4a**)

Yield: 5.8%. $^{1}$H NMR (400 MHz, DMSO-$d_6$): δ 12.53 (1H, s, OH), 10.87 (1H, s, OH), 10.24 (1H, s, OH), 8.03 (2H, d, $J$ = 8.8 Hz), 7.68 (2H, d, $J$ = 8.0 Hz), 7.65 (1H, d, $J$ = 16.4 Hz), 7.52 (2H, d, $J$ = 8.0 Hz), 7.07 (1H, d, $J$ = 16.4 Hz), 6.92(2H, d, $J$ = 8.8 Hz), 6.47 (1H, d, $J$ = 2.0 Hz), 6.21 (1H, d, $J$ = 2.0 Hz), 5.07 (2H, s), 4.36 (1H, s). $^{13}$C NMR (100 MHz, DMSO-$d_6$): δ 194.5, 177.4, 164.2, 161.1, 160.2, 156.3, 155.2, 141.4, 136.2, 134.6, 132.2, 130.5, 128.7, 123.7, 123.3, 120.5, 115.5, 104.0, 98.7, 93.7, 83.2, 83.0, 75.3. HR-ESI-MS *m/z*: found 477.0950, calculated 477.0941 $[M+Na]^+$.

5.1.3.2. 3-O-[(E)-4-(4-(3,3-dimethylbut-1-yn-1-yl)phenyl)-2-oxobut-3-en-1-yl]kaempferol (**4b**)

Yield: 8.1%. $^{1}$H NMR (400 MHz, DMSO-$d_6$): δ 12.54 (1H, s, OH), 10.88 (1H, s, OH), 10.26 (1H, s, OH), 8.04 (2H, d, $J$ = 8.4 Hz), 7.64 (1H, d, $J$ = 16.0 Hz), 7.63 (2H, d, $J$ = 8.0 Hz), 7.39 (2H, d, $J$ = 8.0 Hz), 7.05 (1H, d, $J$ = 16.0 Hz), 6.92(2H, d, $J$ = 8.4 Hz), 6.47 (1H, d, $J$ = 2.0 Hz), 6.21 (1H, d, $J$ = 2.0 Hz), 5.06 (2H, s), 1.30 (9H, s) . $^{13}$C NMR (100 MHz, DMSO-$d_6$): δ 194.4, 177.5, 164.2, 161.1, 160.2, 156.3, 155.2, 141.6, 136.3, 133.6, 131.7, 130.5, 128.6, 125.3, 122.7, 120.5, 115.5, 104.0, 101.0, 98.7, 93.7, 78.8, 75.3, 30.6, 27.7. HR-ESI-MS *m/z*: found 533.1507, calculated 533.1576 $[M+Na]^+$.

5.1.3.3. 3-O-[(E)-4-(4-hydroxybut-1-yn-1-yl)phenyl)-2-oxobut-3-en-1-yl]k

aempferol (**4c**)

Yield: 5.3%. $^{1}$H NMR (400 MHz, DMSO-$d_6$): δ 12.54 (1H, s, OH), 10.89 (1H, s, OH), 10.27 (1H, s, OH), 8.04 (2H, d, $J$ = 8.8 Hz), 7.64 (1H, d, $J$ = 16.0 Hz), 7.64 (2H, d, $J$ = 8.0 Hz), 7.43 (2H, d, $J$ = 8.0 Hz), 7.05 (1H, d, $J$ = 16.0 Hz), 6.92(2H, d, $J$ = 8.8 Hz), 6.47 (1H, d, $J$ = 2.0 Hz), 6.21 (1H, d, $J$ = 2.0 Hz), 5.06 (2H, s), 4.91(1H, m, OH), 3.59(2H, m), 2.58(2H, m). $^{13}$C NMR (100 MHz, DMSO-$d_6$): δ 194.4, 177.5, 164.2, 161.1, 160.2, 156.3, 155.2, 141.6, 136.3, 133.7, 131.8, 130.5, 128.6, 125.3, 122.8, 120.5, 115.5, 104.0, 98.7, 93.7, 91.3, 80.9, 75.3, 59.6, 23.4.HR-ESI-MS *m/z*: found 421.1214, calculated 421.1212 $[M+Na]^+$.

5.1.3.4. 3-O-[(E)-4-(4-(3-hydroxybut-1-yn-1-yl)phenyl)-2-oxobut-3-en-1-yl]kaempferol (**4d**)

Yield: 5.6%. $^{1}$H NMR (400 MHz, DMSO-$d_6$): δ 12.54 (1H, s, OH), 10.89 (1H, s, OH), 10.29 (1H, s, OH), 8.04 (2H, d, $J$ = 8.8 Hz), 7.67 (2H, d, $J$ = 8.4 Hz), 7.65 (1H, d, $J$ = 16.4 Hz), 7.44 (2H, d, $J$ = 8.4 Hz), 7.06 (1H, d, $J$ = 16.4 Hz), 6.92(2H, d, $J$ = 8.8 Hz), 6.47 (1H, d, $J$ = 2.0 Hz), 6.21 (1H, d, $J$ = 2.0 Hz), 5.07 (2H, s), 5.52(1H, d, $J$ = 5.2 Hz, OH ), 4.60(1H, dd, $J_1$ = 5.2 Hz, $J_2$ = 6.8 Hz), 1.38(3H, d, $J$ = 6.8 Hz). $^{13}$C NMR (100 MHz, DMSO-$d_6$): δ 194.5, 177.4, 164.2, 161.1, 160.2, 156.3, 155.2, 141.5, 136.2, 134.0, 131.7, 130.5, 128.7, 124.5, 123.0, 120.5, 115.5, 104.0, 98.7, 95.7, 93.7, 81.9, 75.3, 56.7, 24.5.HR-ESI-MS *m/z*: found 421.1225, calculated 421.1212 $[M+Na]^+$.

5.1.3.5. 3-O-[(E)-4-(4-cyano-2-fluorophenyl)-2-oxobut-3-en-1-yl]kaempfe

rol (**8a**)

Yield: 4.6%. $^{1}$H NMR (400 MHz, DMSO-$d_6$): δ 12.51 (1H, s, OH), 10.90 (1H, s, OH), 10.25 (1H, s, OH), 8.01 (2H, d, $J$ = 8.8 Hz), 7.99-7.76 (3H, m), 7.66 (1H, d, $J$ = 16.4 Hz), 7.27 (1H, d, $J$ = 16.4 Hz), 6.91 (2H, d, $J$ = 8.8 Hz), 6.47 (1H, d, $J$ = 2.0 Hz), 6.21 (1H, d, $J$ = 2.0 Hz), 5.10 (2H, s). $^{13}$C NMR (100 MHz, DMSO-$d_6$): δ 195.0, 177.4, 164.3, 161.2(d, $J$ = 252.0 Hz), 161.1, 160.2, 156.3, 155.2, 136.2, 132.2, 130.4(d, $J$ = 17.3 Hz), 129.0, 127.6, 127.5, 127.1(d, $J$ = 12.0 Hz), 120.4, 120.2(d, $J$ = 25.0 Hz), 117.4, 115.5, 113.8(d, $J$ = 12.0 Hz), 103.9, 98.7, 93.8, 75.6. HR-ESI-MS *m/z*: found 496.0811, calculated 496.0808 [M+Na]+.

5.1.3.6. 3-O-[(E)-4-(5-cyano-2-fluorophenyl)-2-oxobut-3-en-1-yl]kaempfe rol (**8b**)

Yield: 2.2%. $^{1}$H NMR (400 MHz, DMSO-$d_6$): δ 12.52 (1H, s, OH), 10.93 (1H, s, OH), 10.26 (1H, s, OH), 8.03 (2H, d, $J$ = 8.8 Hz), 8.50-7.50 (3H, m), 7.63 (1H, d, $J$ = 16.4 Hz), 7.29 (1H, d, $J$ = 16.4 Hz), 6.90 (2H, d, $J$ = 8.8Hz), 6.47 (1H, d, $J$ = 2.0 Hz), 6.21 (1H, d, $J$ = 2.0 Hz), 5.08 (2H, s). $^{13}$C NMR (100 MHz, DMSO-$d_6$): δ 194.5, 177.4, 164.2, 161.1, 160.2, 156.3, 155.2, 136.1, 134.1, 131.9, 130.5, 126.8, 120.4, 117.7, 115.4, 104.0, 98.7, 93.7, 75.5.HR-ESI-MS *m/z*: found 496.0818, calculated 496.0808 [M+Na]$^{+}$.

5.1.3.7. 3-O-[(E)-4-(4-cyano-3-fluorophenyl)-2-oxobut-3-en-1-yl]kaempfe rol (**8c**)

Yield: 12.6%. $^{1}$H NMR (400 MHz, DMSO-$d_6$): δ 12.52 (1H, s, OH), 10.90

(1H, s, OH), 10.26 (1H, s, OH), 8.03 (2H, d, *J* = 8.8 Hz), 8.00-7.70 (3H, m), 7.67 (1H, d, *J* = 16.4 Hz), 7.25 (1H, d, *J* = 16.4 Hz), 6.91 (2H, d, *J* = 8.8Hz), 6.46 (1H, d, *J* = 2.0 Hz), 6.21 (1H, d, *J* = 2.0 Hz), 5.11 (2H, s). $^{13}$C NMR (100 MHz, DMSO-$d_6$): δ 194.5, 177.4, 164.2, 162.0(d, *J* = 254.0 Hz), 161.1, 160.2, 156.3, 155.2, 142.1(d, *J* = 9.0 Hz), 139.1, 136.2, 134.3, 130.5, 126.7, 125.4(d, *J* = 3.0 Hz), 120.4, 115.6, 115.4(d, *J* = 9.0 Hz), 113.9, 104.0, 101.1(d, *J* = 15.0 Hz), 98.7, 93.7, 75.4. HR-ESI-MS *m/z*: found 496.0823, calculated 496.0808 [M+Na]+.

5.1.3.8. 3-O-[(E)-4-(3-cyano-4-fluorophenyl)-2-oxobut-3-en-1-yl]kaempferol (**8d**)

Yield: 6.1%. $^{1}$H NMR (400 MHz, DMSO-$d_6$): δ 12.53 (1H, s, OH), 10.92 (1H, s, OH), 10.28 (1H, s, OH), 8.04 (2H, d, *J* = 8.8 Hz), 8.35-7.50 (3H, m), 7.65 (1H, d, *J* = 16.4 Hz), 7.16 (1H, d, *J* = 16.4 Hz), 6.90 (2H, d, *J* = 8.8Hz), 6.47 (1H, d, *J* = 2.0 Hz), 6.21 (1H, d, *J* = 2.0 Hz), 5.08 (2H, s). $^{13}$C NMR (100 MHz, DMSO-$d_6$): δ 194.4, 177.4, 164.2, 161.1, 160.2, 156.3, 155.2, 142.1, 139.1, 136.2, 135.8(d, *J* = 9.0 Hz), 133.9, 130.5, 124.4, 120.5, 117.3(d, *J* = 20.0 Hz), 115.4, 113.6, 104.0, 98.7, 93.7, 75.3.HR-ESI-MS *m/z*: found 496.0810, calculated 496.0808 $[M+Na]^{+}$.

5.1.3.9. 3-O-[(E)-4-(5-cyano-3-fluorophenyl)-2-oxobut-3-en-1-yl]kaempferol (**8e**)

Yield: 9.8%. $^{1}$H NMR (400 MHz, DMSO-$d_6$): δ 12.53 (1H, s, OH), 10.90 (1H, s, OH), 10.26 (1H, s, OH), 8.04 (2H, d, *J* = 8.8 Hz), 8.10-7.90 (3H, m),

7.64 (1H, d, *J* = 16.4 Hz), 7.26 (1H, d, *J* = 16.4 Hz), 6.91 (2H, d, *J* = 8.8Hz), 6.46 (1H, d, *J* = 2.0 Hz), 6.21 (1H, d, *J* = 2.0 Hz), 5.10 (2H, s). $^{13}$C NMR (100 MHz, DMSO-$d_6$): δ 194.4, 177.4, 164.2, 162.0(d, *J* = 246.0 Hz), 161.1, 160.2, 156.3, 155.1, 138.8, 138.3(d, *J* = 9.0 Hz), 136.2, 130.5, 128.8, 125.8, 120.4, 120.0(d, *J* = 12.0 Hz), 117.2(d, *J* = 3.0 Hz), 115.4, 113.4(d, *J* = 9.0 Hz), 104.0, 98.6, 93.7, 75.3. HR-ESI-MS *m/z*: found 496.0821, calculated 496.0808 [M+Na]+.

5.1.3.10. 3-O-[(E)-4-(3-cyano-2-chlorophenyl)-2-oxobut-3-en-1-yl]kaempferol (**8f**)

Yield: 2.5%. $^{1}$H NMR (400 MHz, DMSO-$d_6$): δ 12.51 (1H, s, OH), 10.91 (1H, s, OH), 10.26 (1H, s, OH), 8.02(2H, d, *J* = 8.8 Hz), 8.20-7.50 (3H, m), 7.82 (1H, d, *J* = 16.0 Hz), 7.22 (1H, d, *J* = 16.0 Hz), 6.91 (2H, d, *J* = 8.8Hz), 6.47 (1H, s), 6.21 (1H, s), 5.10 (2H, s). $^{13}$C NMR (100 MHz, DMSO-$d_6$): δ 194.4, 177.4, 164.2, 161.1, 160.2, 156.3, 155.2, 136.2, 136.0, 135.7, 133.7, 132.6, 130.5, 128.4, 127.0, 120.4, 115.8, 115.5, 104.0, 98.7, 93.7, 75.6. HR-ESI-MS *m/z*: found 512.0512, calculated 512.0513 [M+Na]+.

5.1.3.11. 3-O-[(E)-4-(5-cyano-2-chlorophenyl)-2-oxobut-3-en-1-yl]kaempferol (**8g**)

Yield: 2.3%. $^{1}$H NMR (400 MHz, DMSO-$d_6$): δ 12.52 (1H, s, OH), 10.92 (1H, s, OH), 10.27 (1H, s, OH), 8.04(2H, d, *J* = 8.8 Hz), 8.50-7.70 (3H, m), 7.79 (1H, d, *J* = 16.4 Hz), 7.33 (1H, d, *J* = 16.4 Hz), 6.90 (2H, d, *J* = 8.8Hz), 6.47 (1H, d, *J* = 2.0 Hz), 6.21 (1H, d, *J* = 2.0 Hz), 5.09 (2H, s). $^{13}$C NMR (100

MHz, DMSO-$d_6$): δ 194.4, 164.2, 161.1, 160.2, 156.3, 155.2, 138.8, 136.2, 134.7, 134.6, 133.4, 132.1, 131.3, 130.5, 127.1, 120.5, 117.6, 115.4, 111.0, 104.0, 93.7, 75.6. HR-ESI-MS *m/z*: found 512.0520, calculated 512.0513 [M+Na]+.

5.1.3.12. 3-O-[(E)-4-(4-cyano-2-(pyrrolidin-1-yl)phenyl)-2-oxobut-3-en-1-yl]kaempferol (**8h**)

Yield: 4.6%. $^1$H NMR (400 MHz, DMSO-$d_6$): δ 12.54 (1H, s, OH), 10.37 (2H, s, OH), 8.02 (2H, d, $J$ = 8.8 Hz), 7.85 (1H, d, $J$ = 16.0 Hz), 7.55 (1H, d, $J$ = 8.0 Hz), 7.21 (1H, d, $J$ = 1.2 Hz), 7.15 (1H, d, $J$ = 8.0 Hz), 6.91 (2H, d, $J$ = 8.8 Hz), 6.84 (1H, d, $J$ = 16.0 Hz), 6.46 (1H, d, $J$ = 2.0 Hz), 6.21 (1H, d, $J$ = 2.0 Hz), 5.04 (2H, s), 3.28(4H, t), 1.87(4H, t). $^{13}$C NMR (100 MHz, DMSO-$d_6$): δ 194.5, 177.4, 164.3, 161.1, 160.2, 156.3, 155.2, 149.6, 140.8, 136.2, 130.5, 130.0, 126.7, 122.9, 120.9, 120.5, 119.0, 118.2, 115.5, 112.6, 104.0, 98.7, 93.7, 75.3, 52.0, 25.2. HR-ESI-MS *m/z*: found 547.1489, calculated 547.1481 [M+Na]+.

5.1.3.13. 3-O-[(E)-4-(5-cyano-2-(pyrrolidin-1-yl)phenyl)-2-oxobut-3-en-1-yl]kaempferol (**8i**)

Yield: 2.5%. $^1$H NMR (400 MHz, DMSO-$d_6$): δ 12.56 (1H, s, OH), 10.90 (1H, s, OH), 10.26 (1H, s, OH), 8.03 (2H, d, $J$ = 8.8 Hz), 7.90 (1H, d, $J$ = 16.0 Hz), 7.83 (1H, d, $J$ = 2.0 Hz), 7.56 (1H, dd, $J_1$ = 2.0 Hz, $J_2$ = 8.8 Hz), 6.91 (2H, d, $J$ = 8.8Hz), 6.85 (1H, d, $J$ = 8.8 Hz), 6.77 (1H, d, $J$ = 16.0 Hz), 6.47 (1H, d, $J$ = 2.0 Hz), 6.21 (1H, d, $J$ = 2.0 Hz), 5.04 (2H, s), 3.40(4H, t),

1.88(4H, t). $^{13}$C NMR (100 MHz, DMSO-$d_6$): δ 194.2, 177.5, 164.2, 161.1, 160.2, 156.3, 155.1, 151.5, 141.3, 136.2, 133.8, 133.5, 130.5, 122.0, 121.2, 120.5, 119.6, 115.5, 115.0, 104.0, 98.6, 98.0, 93.7, 75.1, 51.9, 25.4. HR-ESI-MS *m/z*: found 547.1483, calculated 547.1481 [M+Na]+.

5.1.3.14. 3-O-[(E)-4-(4-cyano-3-(pyrrolidin-1-yl)phenyl)-2-oxobut-3-en-1-yl]kaempferol (**8j**)

Yield: 3.5%. $^{1}$H NMR (400 MHz, DMSO-$d_6$): δ 12.54 (1H, s, OH), 10.91 (1H, s, OH), 10.28 (1H, s, OH), 8.04 (2H, d, *J* = 8.0 Hz), 7.60 (1H, d, *J* = 16.0 Hz), 7.50 (1H, d, *J* = 8.0 Hz), 7.10 (1H, d, *J* = 16.0 Hz), 7.04 (1H, s), 6.99 (1H, d, *J* = 8.0 Hz), 6.91 (2H, d, *J* = 8.0 Hz), 6.47 (1H, s), 6.22 (1H, s), 5.10 (2H, s), 3.54(4H, s), 1.95(4H, s). $^{13}$C NMR (100 MHz, DMSO-$d_6$): δ 194.5, 177.5, 164.2, 161.1, 160.2, 156.3, 155.2, 149.8, 141.6, 139.0, 136.2, 135.6, 130.5, 124.8, 120.6, 120.5, 119.6, 115.8, 115.5, 104.0, 98.6, 94.2, 93.7, 75.3, 49.6, 25.2. HR-ESI-MS *m/z*: found 547.1491, calculated 547.1481 [M+Na]+.

5.1.3.15. 3-O-[(E)-4-(3-cyano-5-(pyrrolidin-1-yl)phenyl)-2-oxobut-3-en-1-yl]kaempferol (**8k**)

Yield: 6.8%. $^{1}$H NMR (400 MHz, DMSO-$d_6$): δ 12.55 (1H, s, OH), 10.89 (1H, s, OH), 10.26 (1H, s, OH), 8.05 (2H, d, *J* = 8.8 Hz), 7.60 (1H, d, *J* = 16.0 Hz), 7.32 (1H, s), 7.13 (1H, d, *J* = 16.0 Hz), 7.09 (1H, s), 6.92 (1H, s), 6.91 (2H, d, *J* = 8.8Hz), 6.47 (1H, d, *J* = 2.0 Hz), 6.21 (1H, d, *J* = 2.0 Hz), 5.10 (2H, s), 3.27(4H, s), 1.96(4H, s). $^{13}$C NMR (100 MHz, DMSO-$d_6$): δ 194.3, 177.5, 164.2, 161.1, 160.2, 156.3, 155.1, 147.8, 141.5, 136.2, 136.0, 130.5,

123.9, 120.5, 119.1, 117.4, 115.8, 115.4, 112.4, 104.0, 98.6, 93.7, 90.6, 75.2, 48.5, 24.9. HR-ESI-MS *m/z*: found 547.1451, calculated 547.1481[M+Na]+.

5.1.3.16. 3-O-[(E)-4-(4-cyano-2-(piperidin-1-yl)phenyl)-2-oxobut-3-en-1-yl ]kaempferol (**8l**)

Yield: 9.6%. $^{1}$H NMR (400 MHz, DMSO-$d_6$): δ 12.54 (1H, s, OH), 10.85 (1H, s, OH), 10.36 (1H, s, OH), 8.03 (2H, d, *J* = 8.8 Hz), 7.85-7.40 (3H, m), 7.76 (1H, d, *J* = 16.4 Hz), 7.12 (1H, d, *J* = 16.4 Hz), 6.92 (2H, d, *J* = 8.8 Hz), 6.46 (1H, d, *J* = 2.0 Hz), 6.21 (1H, d, *J* = 2.0 Hz), 5.07 (2H, s), 2.88(4H, m), 1.66(4H, m), 1.53(2H, m). $^{13}$C NMR (100 MHz, DMSO-$d_6$): δ 194.8, 177.4, 164.2, 161.1, 160.2, 156.3, 155.2, 153.7, 137.6, 136.2, 132.4, 130.5, 128.8, 125.6, 124.4, 122.6, 120.5, 118.7, 115.5, 113.0, 104.0, 98.7, 93.7, 75.4, 53.4, 25.6, 23.4. HR-ESI-MS *m/z*: found 561.1618, calculated 561.1638 [M+Na]+.

5.1.3.17. 3-O-[(E)-4-(5-cyano-2-(piperidin-1-yl)phenyl)-2-oxobut-3-en-1-yl ]kaempferol (**8m**)

Yield: 12.6%. $^{1}$H NMR (400 MHz, DMSO-$d_6$): δ 12.55 (1H, s, OH), 10.89 (1H, s, OH), 10.26 (1H, s, OH), 8.06 (1H, d, *J* = 8.4 Hz), 8.04 (2H, d, *J* = 8.8 Hz), 7.75 (1H, dd, $J_1$ = 2.0 Hz, $J_2$ = 8.4 Hz), 7.65 (1H, d, *J* = 16.4 Hz), 7.17 (1H, d, *J* = 8.4 Hz), 7.12 (1H, d, *J* = 16.4 Hz), 6.91 (2H, d, *J* = 8.8 Hz), 6.47 (1H, d, *J* = 2.0 Hz), 6.21 (1H, d, *J* = 2.0 Hz), 5.07 (2H, s), 2.97 (4H, m), 1.67(4H, m), 1.55(2H, m). $^{13}$C NMR (100 MHz, DMSO-$d_6$): δ 194.6, 177.4, 164.2, 161.1, 160.2, 156.6, 155.1, 137.8, 136.2, 134.3, 132.3, 130.5, 127.6, 123.3, 120.5, 119.0, 118.9, 115.4, 104.0, 103.6, 98.6, 93.7, 75.3, 53.0, 48.6,

25.5, 23.4. HR-ESI-MS *m/z*: found 561.1640, calculated 561.1638 [M+Na]+.

5.1.3.18. 3-O-[(E)-4-(4-cyano-3-(piperidin-1-yl)phenyl)-2-oxobut-3-en-1-yl ]kaempferol (**8n**)

Yield: 10.3%. $^{1}$H NMR (400 MHz, DMSO-$d_6$): δ 12.54 (1H, s, OH), 10.87 (1H, s, OH), 10.26 (1H, s, OH), 8.04 (2H, d, *J* = 8.8 Hz), 7.71 (1H, d, *J* = 8.0 Hz), 7.65 (1H, d, *J* = 16.4 Hz), 7.42(1H, s), 7.34 (1H, d, *J* = 8.0 Hz), 7.17 (1H, d, *J* = 16.4 Hz), 6.91 (2H, d, *J* = 8.8 Hz), 6.47 (1H, d, *J* = 2.0 Hz), 6.22 (1H, d, *J* = 2.0 Hz), 5.10 (2H, s), 3.16(4H, m), 1.68(4H, m), 1.57(2H, m). $^{13}$C NMR (100 MHz, DMSO-$d_6$): δ 194.4, 177.5, 164.2, 161.1, 160.2, 156.4, 155.2, 141.0, 139.7, 136.2, 134.5, 130.5, 125.3, 120.7, 120.5, 119.0, 118.1, 115.5, 105.6, 104.0, 98.7, 93.7, 75.3, 52.4, 25.6, 23.4. HR-ESI-MS *m/z*: found 561.1631, calculated 561.1638 [M+Na]+.

5.1.3.19. 3-O-[(E)-4-(3-cyano-4-(piperidin-1-yl)phenyl)-2-oxobut-3-en-1-yl ]kaempferol (**8o**)

Yield: 4.9%. $^{1}$H NMR (400 MHz, DMSO-$d_6$): δ 12.60 (1H, s, OH), 10.52 (2H, s, OH), 8.09 (2H, d, *J* = 8.8 Hz), 8.07 (1H, s), 7.87 (1H, d, *J* = 8.4 Hz), 7.63 (1H, d, *J* = 16.0 Hz), 7.17 (1H, d, *J* = 8.4 Hz), 7.05 (1H, d, *J* = 16.0 Hz), 6.96 (2H, d, *J* = 8.8 Hz), 6.51 (1H, s), 6.26 (1H, d, *J* = 1.2 Hz), 5.09 (2H, s), 3.30 (4H, m), 1.72(4H, m), 1.63(2H, m). $^{13}$C NMR (100 MHz, DMSO-$d_6$): δ 194.1, 177.5, 164.3, 161.1, 160.2, 156.7, 156.3, 155.1, 140.6, 135.2, 133.6, 130.5, 126.4, 121.1, 120.5, 118.9, 118.1, 115.5, 104.0, 103.1, 98.7, 93.7, 75.2, 51.8, 48.6, 25.5, 23.4. HR-ESI-MS *m/z*: found 561.1621, calculated

561.1638[M+Na]+.

5.1.3.20. 3-O-[(E)-4-(4-cyano-2-morpholinophenyl)-2-oxobut-3-en-1-yl]kaempferol (**8p**)

Yield: 2.3%. $^{1}$H NMR (400 MHz, DMSO-$d_6$): δ 12.53 (1H, s, OH), 10.95 (1H, s, OH), 10.29 (1H, s, OH), 8.02 (2H, d, $J$ = 8.8 Hz), 7.78-7.52 (3H, m), 7.78 (1H, d, $J$ = 16.4 Hz), 7.12 (1H, d, $J$ = 16.4 Hz), 6.91 (2H, d, $J$ = 8.8Hz), 6.47 (1H, d, $J$ = 2.0 Hz), 6.21 (1H, d, $J$ = 2.0 Hz), 5.10 (2H, s), 3.74(4H, t), 2.91(4H, t). $^{13}$C NMR (100 MHz, DMSO-$d_6$): δ 194.8, 177.4, 164.2, 161.1, 160.2, 156.3, 155.2, 152.4, 137.4, 136.2, 132.5, 130.5, 129.1, 126.3, 125.0, 122.7, 120.5, 118.6, 115.5, 113.1, 104.0, 98.7, 93.7, 75.4, 66.1, 52.3. HR-ESI-MS *m/z*: found 563.1432, calculated 563.1430 [M+Na]+.

5.1.3.21. 3-O-[(E)-4-(4-cyano-2-morpholinophenyl)-2-oxobut-3-en-1-yl]kaempferol (**8q**)

Yield: 5.2%. $^{1}$H NMR (400 MHz, DMSO-$d_6$): δ 12.55 (1H, s, OH), 10.90 (1H, s, OH), 10.27 (1H, s, OH), 8.09 (1H, d, $J$ = 1.6 Hz), 8.02 (2H, d, $J$ = 8.8 Hz), 7.80 (1H, dd, $J_1$ = 1.6 Hz, $J_2$ = 8.4 Hz), 7.68 (1H, d, $J$ = 16.4 Hz), 7.21 (1H, d, $J$ = 8.4 Hz), 7.12 (1H, d, $J$ = 16.4 Hz), 6.91 (2H, d, $J$ = 8.8Hz), 6.47 (1H, d, $J$ = 2.0 Hz), 6.21 (1H, d, $J$ = 2.0 Hz), 5.07 (2H, s), 3.75(4H, t), 2.99(4H, t). $^{13}$C NMR (100 MHz, DMSO-$d_6$): δ 194.7, 177.4, 164.2, 161.1, 160.2, 156.3, 155.5, 155.1, 137.6, 136.2, 134.5, 132.6, 130.5, 127.8, 124.1, 120.5, 119.5, 118.8, 115.4, 104.4, 104.0, 98.7, 93.7, 75.3, 66.0, 52.0. HR-ESI-MS *m/z*: found 563.1426, calculated 563.1430 [M+Na]+.

5.1.3.22. 3-O-[(E)-4-(5-cyano-2-morpholinophenyl)-2-oxobut-3-en-1-yl]kaempferol (**8r**)

Yield: 1.8%. $^{1}$H NMR (400 MHz, DMSO-$d_6$): δ 12.54 (1H, s, OH), 10.94 (1H, s, OH), 10.27 (1H, s, OH), 8.04 (2H, d, $J$ = 8.8 Hz), 7.76 (1H, d, $J$ = 8.0 Hz), 7.66 (1H, d, $J$ = 16.4 Hz), 7.46 (1H, d, $J$ = 0.8 Hz), 7.40 (1H, dd, $J_1$ = 0.8 Hz, $J_2$ = 8.0 Hz), 7.19 (1H, d, $J$ = 16.4 Hz), 6.91 (2H, d, $J$ = 8.8Hz), 6.47 (1H, d, $J$ = 2.0 Hz), 6.21 (1H, d, $J$ = 2.0 Hz), 5.11 (2H, s), 3.77(4H, t), 3.18(4H, t). $^{13}$C NMR (100 MHz, DMSO-$d_6$): δ 194.4, 177.4, 164.2, 161.1, 160.2, 155.2, 140.9, 139.9, 136.2, 134.7, 130.5, 125.5, 121.5, 120.5, 118.9, 118.0, 115.5, 105.6, 104.0, 98.7, 93.7, 75.3, 66.1, 51.3. HR-ESI-MS *m/z*: found 563.1439, calculated 563.1430 [M+Na]+.

5.1.3.23. 3-O-[(E)-4-(3-cyano-4-morpholinophenyl)-2-oxobut-3-en-1-yl]kaempferol (**8s**)

Yield: 6.8%. $^{1}$H NMR (400 MHz, DMSO-$d_6$): δ 12.55 (1H, s, OH), 10.91 (1H, s, OH), 10.27 (1H, s, OH), 8.08 (1H, d, $J$ = 2.0 Hz), 8.05 (2H, d, $J$ = 8.8 Hz), 7.89 (1H, dd, $J_1$ = 2.0 Hz, $J_2$ = 8.8 Hz), 7.60 (1H, d, $J$ = 16.0 Hz), 7.17 (1H, d, $J$ = 8.8 Hz), 7.04 (1H, d, $J$ = 16.0 Hz), 6.91 (2H, d, $J$ = 8.8Hz), 6.47 (1H, d, $J$ = 2.0 Hz), 6.21 (1H, d, $J$ = 2.0 Hz), 5.05 (2H, s), 3.76(4H, t), 3.28(4H, t). $^{13}$C NMR (100 MHz, DMSO-$d_6$): δ 194.2, 177.5, 164.2, 161.1, 160.2, 156.3, 155.8, 155.2, 140.3, 136.2, 135.1, 133.9, 130.5, 127.4, 121.7, 120.5, 119.0, 117.9, 115.5, 104.0, 103.5, 98.6, 93.7, 75.2, 65.9, 50.8. HR-ESI-MS *m/z*: found 563.1421, calculated 563.1430 [M+Na]+.

5.1.3.24. 3-O-[(E)-4-(2-(4-(tert-butoxycarbonyl)piperazin-1-yl)-4-cyanophenyl)-2-oxobut-3-en-1-yl]kaempferol (**8t**)

Yield: 13.0%. $^{1}$H NMR (400 MHz, DMSO-$d_6$): δ 12.52 (1H, s, OH), 10.89 (1H, s, OH), 10.26 (1H, s, OH), 8.02 (2H, d, $J$ = 8.8 Hz), 7.80-7.50 (3H, m), 7.81 (1H, d, $J$ = 16.4 Hz), 7.11 (1H, d, $J$ = 16.4 Hz), 6.91 (2H, d, $J$ = 8.8Hz), 6.46 (1H, d, $J$ = 2.0 Hz), 6.21 (1H, d, $J$ = 2.0 Hz), 5.09 (2H, s), 3.48(4H, t), 2.88(4H, t), 1.41(9H, s). $^{13}$C NMR (100 MHz, DMSO-$d_6$): δ 194.8, 177.4, 164.2, 161.1, 160.2, 156.2, 155.2, 153.9, 152.3, 137.4, 136.2, 132.7, 130.5, 129.0, 126.4, 125.3, 123.1, 120.5, 118.5, 115.5, 113.0, 104.0, 98.6, 93.7, 79.1, 75.3, 51.8, 48.6, 28.0. HR-ESI-MS *m/z*: found 662.2111, calculated 662.2114[M+Na]+.

5.1.3.25. 3-O-[(E)-4-(2-(4-(tert-butoxycarbonyl)piperazin-1-yl)-5-cyanophenyl)-2-oxobut-3-en-1-yl]kaempferol (**8u**)

Yield: 16.5%. $^{1}$H NMR (400 MHz, DMSO-$d_6$): δ 12.54 (1H, s, OH), 10.46 (2H, s, OH), 8.10 (1H, d, $J$ = 1.2 Hz), 8.03 (2H, d, $J$ = 8.8 Hz), 7.80 (1H, dd, $J_1$ = 1.2 Hz, $J_2$ = 8.4 Hz), 7.68 (1H, d, $J$ = 16.4 Hz), 7.21 (1H, d, $J$ = 8.4 Hz), 7.11 (1H, d, $J$ = 16.4 Hz), 6.91 (2H, d, $J$ = 8.8Hz), 6.47 (1H, d, $J$ = 2.0 Hz), 6.21 (1H, d, $J$ = 2.0 Hz), 5.09 (2H, s), 3.49(4H, t), 2.96(4H, t), 1.41(9H, s). $^{13}$C NMR (100 MHz, DMSO-$d_6$): δ 194.7, 177.4, 164.3, 161.1, 160.2, 156.3, 155.4, 155.1, 153.8, 137.5, 136.2, 134.5, 132.5, 130.5, 128.0, 124.4, 120.5, 119.8, 118.7, 115.4, 104.6, 104.0, 98.7, 93.7, 79.1, 75.2, 62.7, 51.5, 28.0. HR-ESI-MS *m/z*: found 662.2121, calculated 662.2114 [M+Na]+.

### 5.1.4. General procedure for compound 10 synthesis

Derivatives **8t** or **8u** (10 mg) were mixed in MeOH (1.5 ml) and added with 80 μl of concentrated HCL in an ice bath. The mixture was stirred for 15 h at room temperature until TLC ($CH_2Cl_2$: MeOH, 95:5) indicated that the starting material had disappeared. Under pressure, the solvent was removed from the reaction mixture to produce a yellow solid.

5.1.4.1. 3-O-[(E)-4-(4-cyano-2-(piperazin-1-yl)phenyl)-2-oxobut-3-en-1-yl ]kaempferol hydrochlorate (**10a**)

Yield: 96%. $^1$H NMR (400 MHz, DMSO-$d_6$): δ 12.52 (1H, s, OH), 11.00 (1H, s, OH), 10.35 (1H, s, OH), 9.14 (2H, s, NH), 8.02 (2H, d, $J$ = 8.0 Hz), 7.80-7.50 (3H, m), 7.79 (1H, d, $J$ = 16.4 Hz), 7.13 (1H, d, $J$ = 16.4 Hz), 6.93 (2H, d, $J$ = 8.0 Hz), 6.50 (1H, s), 6.23 (1H, s), 5.10 (2H, s), 3.26(4H, t), 3.15(4H, t). $^{13}$C NMR (100 MHz, DMSO-$d_6$): δ 194.8, 177.4, 164.3, 161.1, 160.3, 156.3, 155.2, 151.3, 137.0, 136.2, 132.7, 130.5, 129.2, 127.0, 125.7, 123.1, 120.5, 115.5, 113.1, 104.0, 98.7, 93.8, 75.4, 48.9, 42.9. HR-ESI-MS *m/z*: found 562.1588, calculated 562.1590 [M+Na-HCl]+.

5.1.4.2. 3-O-[(E)-4-(5-cyano-2-(piperazin-1-yl)phenyl)-2-oxobut-3-en-1-yl ]kaempferol hydrochlorate (**10b**)

Yield: 94%. $^1$H NMR (400 MHz, DMSO-$d_6$): δ 12.54 (1H, s, OH), 11.02 (1H, s, OH), 10.35 (1H, s, OH), 9.22 (2H, s, NH), 8.15 (1H, d, $J$ = 1.6 Hz), 8.04 (2H, d, $J$ = 8.8 Hz), 7.84 (1H, dd, $J_1$ = 1.6 Hz, $J_2$ = 8.4 Hz), 7.66 (1H, d, $J$ = 16.0 Hz), 7.29 (1H, d, $J$ = 8.4 Hz), 7.14 (1H, d, $J$ = 16.0 Hz), 6.93 (2H, d, $J$ =

8.8Hz), 6.51 (1H, d, $J$ = 2.0 Hz), 6.24 (1H, d, $J$ = 2.0 Hz), 5.10 (2H, s), 3.27(4H, t), 3.23(4H, t). $^{13}$C NMR (100 MHz, DMSO-$d_6$): δ 194.6, 177.5, 164.3, 161.1, 160.3, 156.3, 155.2, 154.5, 137.0, 136.2, 134.6, 132.6, 130.5, 128.2, 124.8, 120.5, 119.9, 118.6, 115.5, 105.3, 104.0, 98.7, 93.8, 75.3, 48.6, 42.7. HR-ESI-MS *m/z*: found 562.1562, calculated 562.1590 [M+Na-HCl]+.

**5.2. Cell culture**

Human hepatocellular carcinoma cells (HepG2) were obtained from American Type Culture Collection. The HepG2 cells were cultured in Dulbecco's modified Eagle's medium (DMEM-F12 medium containing with 2.5% fetal bovine serum (FBS) and antibiotics (gentamicin, penicillin, and streptomycin (50 mg/L)). Cells were grown at 37 °C in a humidified atmosphere of 5% $CO_2$. One day after plating, the medium was changed to DMEM containing 5.5 mM D-glucose, 2 mM glutamine, and FBS, and the culture was continued. Subsequently, the experimental treatments were carried out for the indicated periods with various concentrations of glucose in serum-free media for 24 h.

**5.3. Cytotoxicity tests**

To evaluate cell viability of HepG2 cells, they were seeded at $1 \times 10^4$ cells/ml in 96 well culture plates and incubated for 24 h at 37 °C in a humidified atmosphere containing 5% $CO_2$. Flavonoid derivatives were added at 1–25

μM and incubated for a further 24 h. An MTT (2,3-bis-(2-methoxy-4-nitro-5-sulfophenyl)-2H-tetrazolium-5-carboxanilide) assay was used to test cell viability, in which 20% of MTT (purchased from Sigma Aldrich, Gillingham, UK, as a working solution at 5 mg/ml in phosphate-buffered saline (PBS) was added to the cells and incubated for 4 h at 37 °C in a humidified atmosphere containing 5% $CO_2$. The cells were then solubilized in 100% dimethyl sulfoxide (DMSO) for 5 min. The absorbance was measured using microplate reader (BioTek, Winooski, VT, USA) at 570 nm.

**5.4. Glucose uptake assay**

The glucose uptake rate was measured using a fluorescent D-glucose derivative, 2-NBDG, according to a published procedure with some modifications [29]. For fluorescent microplate reader measurement of the 2-NBDG uptake level, $1 \times 10^4$ HepG2 cells per well were seeded in a black clear-bottomed 96-well culture plate (Corning Inc., Corning, NY, USA). The cells were pre-incubated with flavonoid derivatives. After 24 h, the cells were cultured in serum-free low-glucose (5.5 mM) culture medium for 3 h before the addition of insulin and 2-NBDG. 2-NBDG uptake was measured using a fluorescent microplate reader (BioTek) using excitation and emission wavelengths of 488 and 520 nm, respectively.

### 5.5. Gluconeogenesis assays

HepG2 cells were seeded in 24-well plates ($2 \times 10^5$ cells per well). The cells were pre-incubated with flavonoid derivatives for 24 h. The positive control was metformin at 1.0 mM. On the day of the assay, glucose production buffer comprising glucose-free DMEM (pH 7.4), without phenol red (Invitrogen, Madrid, Spain), containing 20 mM sodium lactate and 2 mM sodium pyruvate was used to replace the culture medium, as described previously[30, 31]. Medium was collected after incubation for 3 h incubation, and the glucose concentration was measured using a colorimetric glucose assay kit (Sigma, Madrid, Spain). The total protein content determined using whole-cell lysates was used to normalize the readings. The bicinchoninic acid protein (BCA) assay kits (Nanjing Jiancheng Bioengineering Institute, Nanjing, China) for the whole-cell lysates.

### 5.6. Glycogen Content Assay

Each group of HepG2 cells was counted, and then the glycogen content of the cells was detected using the anthrone−sulfuric acid method in a glycogen assay kit. Briefly, HepG2 cells were seeded in 6-well plates ($2 \times 10^6$ cells per well). The cells were pre-incubated with flavonoid derivatives for 24 h. On the day of the assay, HepG2 cells were digested and centrifuged, and the precipitates were transferred to glass tubes with 0.225 mL of alkaline liquor. Samples were incubated in boiling water for 20 min, and then 0.1 mL of

hydrolysate was diluted with distilled water and 2 mL of a color-substrate solution, according to the manufacturer's instructions. Subsequently, samples were incubated in boiling water for 5 min. Thereafter, the OD value of each group was determined at 620 nm using a microplate reader (BioTek). The cell total glycogen content was calculated and expressed as milligrams per $10^6$ cells.

### 5.7. Glycolysis assay

The HepG2 cultured in 96-well plates were treated with flavonoid derivatives in DMEM supplemented with 0.25% BSA for 24 h. The positive control was insulin at 100 nM. The lactate concentration in the medium was measured using a lactate reagent kit (Shanghai Juchuang Biotechnology Corporation, Shanghai, China).

### 5.8. Western blotting analysis

Cells were lysed at 4 °C in a buffer containing 25 mM HEPES (pH 7.5), 0.3 M NaCl, 1.5 mM $MgCl_2$, 0.2 mM EDTA, 0.5 mM dithiothreitol, 0.1% Triton X-100, 200 mM b-glycerolphosphate, 0.1 mM $Na_3VO_4$, 2 μg/mL leupeptin, and 1 mM phenylmethylsulfonylfluoride. The supernatants were collected, assayed for their protein concentration by using a Bio-Rad (Bio-Rad, Madrid, Spain) protein assay kit (according to the manufacturer's specifications), aliquoted, and stored at −80 °C until use. The protein concentrations in the

samples were measured using the Bio-Rad protein assay reagent. Equal amounts of protein samples (60 mg/lane) were separated using 10% sodium dodecylsulfate-polyacrylamide gel electrophoresis (SDS-PAGE) and transferred to a polyvinylidene fluoride membrane (Millipore, Bedford, MA, USA). Nonfat milk (5%) in TBS containing 0.1% Tween 20 (TBS-T) was used to block the membranes for 1 h. The membranes were then incubated at 4 °C overnight with primary antibodies recognizing p-AMPK, AMPK, PEPCK, G6P, and β-actin (Cell Signaling Technology, Inc., Danvers, MA, USA). The membranes were then incubated with horseradish peroxidase-conjugated secondary antibodies. The enhanced chemiluminescence western blotting detection system (GE Healthcare Life Science, Buckinghamshire, UK) was used to visualize the immunoreactive proteins on the membranes.

**5.9. Measurements of intracellular ATP and AMP levels**

Intracellular ATP and AMP contents were measured using high performance liquid chromatography (HPLC) [32]. In brief, HepG2 cells grown in the presence or absence of **10b** were subjected to two rounds of washing with cold PBS and then lysed using 0.5 M perchloric acid. The lysate was briefly sonicated and then neutralized with 2 M KOH. After centrifugation, the supernatant was analyzed using HPLC (Agilent) with an LC-18T reverse-phase column (Agilent) at a flow rate of 1.0 ml/min, and the absorbance at 280 nm was recorded. Each elution peak was compared with

AMP and ATP standards (National Institute for Food and Drug Control, Beijing, China) to confirm its identity. The ATP or AMP concentrations were determined using an ATP or AMP standard curve. All experiments were repeated at least three times.

**Acknowledgments**

This work was supported by the National Natural Science Foundation of China (NSFC) [grant number 81373297]; and the Tianjin Research Program of Applied Basic and Cutting-edge Technologies [grant number 12JCZDJC25900, 18JCQNJC13800].

**Declarations of interest**

None

## Reference

[1] R.N. Bergman, F. Piccinini, M. Kabir, M. Ader, Novel aspects of the role of the liver in carbohydrate metabolism, Metabolism, (2019).

[2] M.F. Hopgood, F.J. Ballard, Synthesis and degradation of phosphoenolpyruvate carboxylase in rat liver and adipose tissue. Changes during a starvation-re-feeding cycle, Biochem J, 134 (1973) 445-453.

[3] M.B. Weinberg, M.F. Utter, Effect of streptozotocin-induced diabetes mellitus on the turnover of rat liver pyruvate carboxylase and pyruvate dehydrogenase, Biochem J, 188 (1980) 601-608.

[4] D.G. Hardie, AMPK: a target for drugs and natural products with effects on both diabetes and cancer, Diabetes, 62 (2013) 2164-2172.

[5] N. Qin, C.B. Li, M.N. Jin, L.H. Shi, H.Q. Duan, W.Y. Niu, Synthesis and biological activity of novel tiliroside derivants, Eur J Med Chem, 46 (2011) 5189-5195.

[6] N. Qin, Y. Chen, M.N. Jin, C. Zhang, W. Qiao, X.L. Yue, H.Q. Duan, W.Y. Niu, Anti-obesity and anti-diabetic effects of flavonoid derivative (Fla-CN) via microRNA in high fat diet induced obesity mice, Eur J Pharm Sci, 82 (2016) 52-63.

[7] K. Zumbansen, A. Döhring, B. List, Morpholinium Trifluoroacetate-Catalyzed Aldol Condensation of Acetone with both Aromatic and Aliphatic Aldehydes, Advanced Synthesis & Catalysis, 352 (2010) 1135-1138.

[8] R. Wilcken, M.O. Zimmermann, A. Lange, A.C. Joerger, F.M. Boeckler, Principles and applications of halogen bonding in medicinal chemistry and chemical biology, J Med Chem, 56 (2013) 1363-1388.

[9] G. Zhou, R. Myers, Y. Li, Y. Chen, X. Shen, J. Fenyk-Melody, M. Wu, J. Ventre, T. Doebber, N. Fujii, N. Musi, M.F. Hirshman, L.J. Goodyear, D.E. Moller, Role of AMP-activated protein kinase in mechanism of metformin action, J Clin Invest, 108 (2001) 1167-1174.

[10] N. Turner, J.Y. Li, A. Gosby, S.W. To, Z. Cheng, H. Miyoshi, M.M. Taketo, G.J. Cooney, E.W. Kraegen, D.E. James, L.H. Hu, J. Li, J.M. Ye, Berberine and its more biologically available derivative, dihydroberberine, inhibit mitochondrial respiratory complex I: a mechanism for the action of berberine to activate AMP-activated protein kinase and improve insulin action, Diabetes, 57 (2008) 1414-1418.

[11] J.R. Gledhill, M.G. Montgomery, A.G. Leslie, J.E. Walker, Mechanism of inhibition of bovine F1-ATPase by resveratrol and related polyphenols, Proc Natl Acad Sci U S A, 104 (2007) 13632-13637.

[12] E. Vitaku, D.T. Smith, J.T. Njardarson, Analysis of the structural diversity, substitution patterns, and frequency of nitrogen heterocycles among U.S. FDA approved pharmaceuticals, J Med Chem, 57 (2014) 10257-10274.

[13] M. Shaquiquzzaman, G. Verma, A. Marella, M. Akhter, W. Akhtar, M.F. Khan, S. Tasneem, M.M. Alam, Piperazine scaffold: A remarkable tool in generation of diverse pharmacological agents, Eur J Med Chem, 102 (2015) 487-529.

[14] G.R. Steinberg, D. Carling, AMP-activated protein kinase: the current landscape for drug development, Nat Rev Drug Discov, (2019).

[15] J.E. Sullivan, K.J. Brocklehurst, A.E. Marley, F. Carey, D. Carling, R.K. Beri, Inhibition of lipolysis and lipogenesis in isolated rat adipocytes with AICAR, a cell-permeable activator of AMP-activated protein kinase, FEBS Lett, 353 (1994) 33-36.

[16] J.M. Corton, J.G. Gillespie, S.A. Hawley, D.G. Hardie, 5-aminoimidazole-4-carboxamide ribonucleoside. A specific method for activating AMP-activated protein kinase in intact cells?, Eur J

Biochem, 229 (1995) 558-565.
[17] M.R. Owen, E. Doran, A.P. Halestrap, Evidence that metformin exerts its anti-diabetic effects through inhibition of complex 1 of the mitochondrial respiratory chain, Biochem J, 348 Pt 3 (2000) 607-614.
[18] Y.S. Lee, W.S. Kim, K.H. Kim, M.J. Yoon, H.J. Cho, Y. Shen, J.M. Ye, C.H. Lee, W.K. Oh, C.T. Kim, C. Hohnen-Behrens, A. Gosby, E.W. Kraegen, D.E. James, J.B. Kim, Berberine, a natural plant product, activates AMP-activated protein kinase with beneficial metabolic effects in diabetic and insulin-resistant states, Diabetes, 55 (2006) 2256-2264.
[19] J. Ahn, H. Lee, S. Kim, J. Park, T. Ha, The anti-obesity effect of quercetin is mediated by the AMPK and MAPK signaling pathways, Biochem Biophys Res Commun, 373 (2008) 545-549.
[20] B. Xiao, M.J. Sanders, D. Carmena, N.J. Bright, L.F. Haire, E. Underwood, B.R. Patel, R.B. Heath, P.A. Walker, S. Hallen, F. Giordanetto, S.R. Martin, D. Carling, S.J. Gamblin, Structural basis of AMPK regulation by small molecule activators, Nat Commun, 4 (2013) 3017.
[21] W. Niu, P.J. Bilan, S. Ishikura, J.D. Schertzer, A. Contreras-Ferrat, Z. Fu, J. Liu, S. Boguslavsky, K.P. Foley, Z. Liu, J. Li, G. Chu, T. Panakkezhum, G.D. Lopaschuk, S. Lavandero, Z. Yao, A. Klip, Contraction-related stimuli regulate GLUT4 traffic in C2C12-GLUT4myc skeletal muscle cells, Am J Physiol Endocrinol Metab, 298 (2010) E1058-1071.
[22] C.P. Miinea, H. Sano, S. Kane, E. Sano, M. Fukuda, J. Peranen, W.S. Lane, G.E. Lienhard, AS160, the Akt substrate regulating GLUT4 translocation, has a functional Rab GTPase-activating protein domain, Biochem J, 391 (2005) 87-93.
[23] S.R. Hargett, N.N. Walker, S.R. Keller, Rab GAPs AS160 and Tbc1d1 play nonredundant roles in the regulation of glucose and energy homeostasis in mice, Am J Physiol Endocrinol Metab, 310 (2016) E276-288.
[24] R. Bergeron, S.F. Previs, G.W. Cline, P. Perret, R.R. Russell, 3rd, L.H. Young, G.I. Shulman, Effect of 5-aminoimidazole-4-carboxamide-1-beta-D-ribofuranoside infusion on in vivo glucose and lipid metabolism in lean and obese Zucker rats, Diabetes, 50 (2001) 1076-1082.
[25] P.A. Lochhead, I.P. Salt, K.S. Walker, D.G. Hardie, C. Sutherland, 5-aminoimidazole-4-carboxamide riboside mimics the effects of insulin on the expression of the 2 key gluconeogenic genes PEPCK and glucose-6-phosphatase, Diabetes, 49 (2000) 896-903.
[26] R.M. O'Brien, D.K. Granner, Regulation of gene expression by insulin, Physiol Rev, 76 (1996) 1109-1161.
[27] M. Foretz, N. Ancellin, F. Andreelli, Y. Saintillan, P. Grondin, A. Kahn, B. Thorens, S. Vaulont, B. Viollet, Short-term overexpression of a constitutively active form of AMP-activated protein kinase in the liver leads to mild hypoglycemia and fatty liver, Diabetes, 54 (2005) 1331-1339.
[28] M. Gazvoda, M. Virant, B. Pinter, J. Kosmrlj, Mechanism of copper-free Sonogashira reaction operates through palladium-palladium transmetallation, Nat Commun, 9 (2018) 4814.
[29] R.G. O'Neil, L. Wu, N. Mullani, Uptake of a fluorescent deoxyglucose analog (2-NBDG) in tumor cells, Mol Imaging Biol, 7 (2005) 388-392.
[30] Q.F. Collins, H.-Y. Liu, J. Pi, Z. Liu, M.J. Quon, W. Cao, Epigallocatechin-3-gallate (EGCG), A Green Tea Polyphenol, Suppresses Hepatic Gluconeogenesis through 5′-AMP-activated Protein Kinase, Journal of Biological Chemistry, 282 (2007) 30143-30149.
[31] A.B. Granado-Serrano, M.A. Martín, G. Haegeman, L. Goya, L. Bravo, S. Ramos, Epicatechin induces NF-κB, activator protein-1 (AP-1) and nuclear transcription factor erythroid 2p45-related factor-2 (Nrf2) via phosphatidylinositol-3-kinase/protein kinase B (PI3K/AKT) and extracellular regulated kinase (ERK) signalling in HepG2 cells, British Journal of Nutrition, 103 (2009) 168-179.

[32] S.S. Xing, X.Y. Yang, T. Zheng, W.J. Li, D. Wu, J.Y. Chi, F. Bian, X.L. Bai, G.J. Wu, Y.Z. Zhang, C.T. Zhang, Y.H. Zhang, Y.S. Li, S. Jin, Salidroside improves endothelial function and alleviates atherosclerosis by activating a mitochondria-related AMPK/PI3K/Akt/eNOS pathway, Vascul Pharmacol, 72 (2015) 141-152.

Graphical abstract

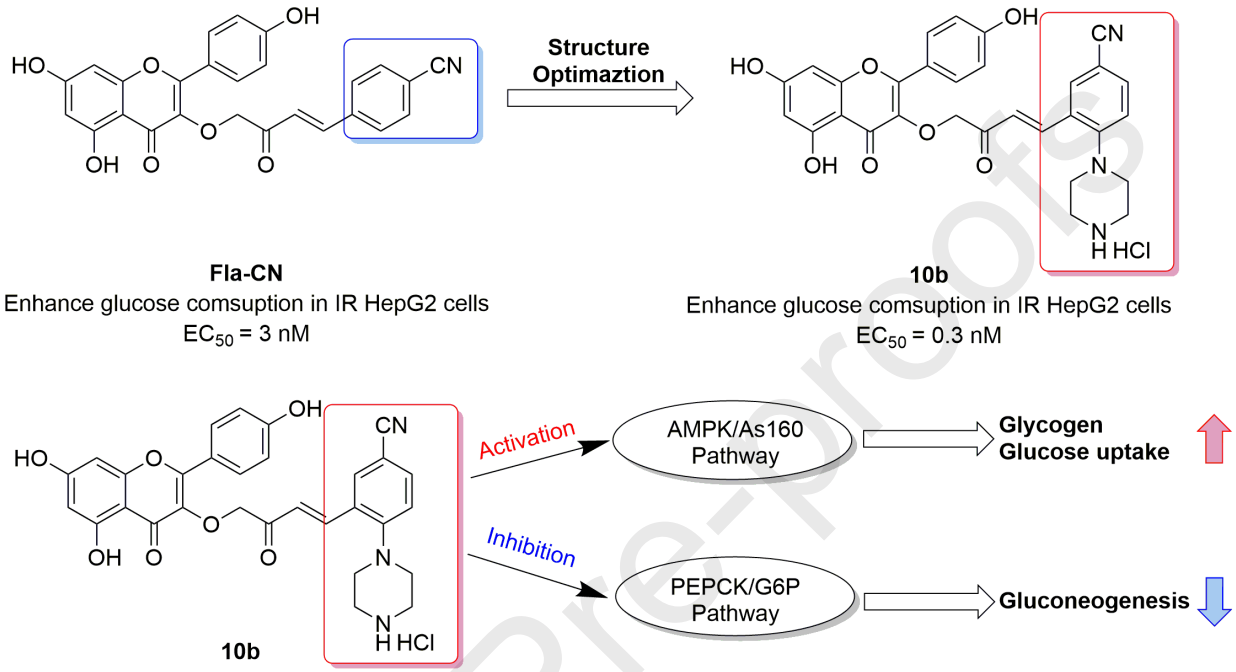

Highlight

Discovery of a semi-synthesized flavonoid derivative **10b** which could enhance glucose consumption in IR HepG2 cells.

Flavonoid derivative **10b** could increase the glycogen content and glucose uptake and inhibited the gluconeogenesis in HepG2 cells.

Flavonoid derivative **10b** markedly enhanced the phosphorylation of AMPK and AS160 and reduced the levels of the gluconeogenesis key enzymes PEPCK and G6P in HepG2 cells.

**Conflict of interest**

The authors report that they have no declarations of interest.